TECHNOLOGICAL CHALLENGES IN THE FABRICATION OF MOS_2/DIAMOND HETEROSTRUCTURES

[1,2]Marian VARGA, [1]Michaela SOJKOVA, [1,3]Jana HRDA, [1]Peter HUTAR, [1,3]Saviz PARSA SAEB, [1]Gabriel VANKO, [1]Lenka PRIBUSOVA SLUSNA, [2]Lukas ONDIC, [2]Jan FAIT, [2]Alexander KROMKA, [1]Martin HULMAN

[1]Institute of Electrical Engineering, Slovak Academy of Sciences, Bratislava, Slovakia, EU

[2]Institute of Physics, Czech Academy of Sciences, Prague, Czech Republic, EU

[3]Faculty of Electrical Engineering and Information Technology, Slovak University of Technology, Bratislava, Slovakia, EU

https://doi.org/10.37904/nanocon.2022.4586

Abstract

Nowadays, 2D materials are one of the most studied classes of materials. In addition to the most famous graphene, progress has been achieved in studying and using fundamental properties of transition metal dichalcogenides (TMD). Complementary, diamond as a representative of 3D materials has gained a reputation as an extremely versatile material due to its extraordinary combination of physical/chemical/electrical/optical properties. Besides these particular forms of 2D and 3D materials, their heterostructures have become very attractive due to new phenomena and functions (bandgap engineering, enhanced charge transport, optical interaction, etc.). However, individual technological procedures are still minimally investigated and described. Here, we will demonstrate a proof-of-concept for the preparation of MoS_2/diamond heterostructures, where two different strategies were employed: a) growth of MoS_2 layers on diamond films, and b) growth of diamond films on Si/MoS_2 substrates. Considering the growth conditions for MoS_2 and diamond materials, heterostructures based on MoS_2 on diamond can be prepared more easily. Regardless of the diamond film's morphology, the grown MoS_2 layer simply copies the diamond surface and does not damage the diamond film. However, the heterostructure in the configuration of diamond on MoS_2 is a highly challenging task. It was found experimentally that the combination of deposition temperature and aggressive chemical-plasma environment during diamond growth places high demands on the resistance and stability of MoS_2 layers.

Keywords: Transition metal dichalcogenides, diamond, heterostructures, chemical vapor deposition

1. INTRODUCTION

Two-dimensional (2D) materials have been one of the most extensively studied classes of materials due to their unusual physical properties. Besides the most known graphene, in recent years, progress has been achieved in exploring and using the fundamental properties of the transition metal dichalcogenides (TMD). Depending on the combination of transition metal (e.g. Mo, Pt, W, Ni or Ti) and chalcogen (e.g. S, Se, or Te), the group of TMD materials has roughly more than 60 different members which exhibit various properties [1]. These properties make them highly attractive for fundamental studies of novel physical phenomena as well as for a wide range of applications. In addition, heterostructures of two or more atomically thin materials with a large variety of bandgaps and electron affinities may have properties suitable for electronic and photonic applications [2,3]. MoS_2 is recently one of the most studied TMDs composed of covalently bonded S-Mo-S sheets which are bound by weak van der Waals forces [4]. MoS_2 is a semiconductor with an indirect bandgap of about 1.3 eV, however, the monolayer MoS_2 is a direct gap semiconductor with a bandgap of 1.8 eV. This is, in particular, important for photovoltaic and photocatalytic applications due to its strong absorption in the solar spectral region. However, properly used fabrication methods and growth conditions are crucial aspects

that tailor the crystallographic structure, material quality, number of layers, and thus the properties of the TMD material in a wide range [5].

Conversely, diamond as a representative of 3D materials has gained a reputation as an extremely versatile material due to its extraordinary combination of physical/chemical/electrical/optical properties. These fascinating properties make diamond an ideal material for a wide range of applications [6]. Although single-crystal diamond is a better candidate than polycrystalline diamond films, its production and machining of single-crystals are quite cumbersome [7]. In contrast, polycrystalline diamond thin films with desired properties (thickness, morphology, crystal size, etc.) can be easily deposited at low cost on a wide range of substrates and also over large areas. Similar to TMD materials, the diamond properties (bulk or surface) can be significantly controlled by the growth conditions and post-growth processing [8].

Besides the individual forms of 2D materials and/or 3D diamond crystals, their heterostructures have also attracted the research community's attention due to novel phenomena and functionalities at artificial hetero-interfaces, and the enhancement of advantageous properties that further expand the applicability fields [9]. For instance, a computational study of the thermal stability of the MoS_2/diamond structure suggests that the single-layer MoS_2 film on diamond can be used as a field-effect transistor or a heat-generating gate junction heterostructure up to the temperature of 550 K [10]. In addition, a successful horizontal or vertical growth of a MoS_2 layer on a thick well-faceted microcrystalline diamond film has already been demonstrated by our group [4]. However, CVD diamond growth on TMD materials is a challenging issue due to thermal expansion differences, crystallographic mismatches and the aggressiveness of CVD conditions. Here, we focused on the preparation of MoS_2/diamond heterostructures in two different configurations and highlighted the growth mechanism and technological obstacles.

2. MATERIALS AND METHODS

In this work, MoS_2 was chosen as a representative TMD material. The MoS_2 layers were prepared by sulfurization of sputtered Mo layers (4 nm thick) in a custom-designed one-zone CVD chamber (**Figure 1a**) at 800 °C for 30 min. The Mo-coated substrate was placed in the center of the tube furnace along with sulfur powder (3 g, purity of 99,999 %). Sulfurization took place at atmospheric pressure in a constant N_2 flow.

For the diamond growth, a pulsed MW plasma CVD system with a linear antenna arrangement (Roth&Rau AK400) was selected (**Figure 1b**). This CVD system reveals a homogeneous “cold” plasma distribution at a low working pressure (units of Pa) over a water-cooled graphite substrate holder of 30 × 20 cm^2. Two gas compositions of CH_4:CO_2:H_2 with flow rates of 5:20:50 sccm and 10:40:50 sccm were tested. Apart from the gas composition, the deposition parameters were the same for both depositions, i.e. deposition time t = 20 hours, working pressure p = 0.15 mbar, microwave power P = 2×1700 W (ON/OFF duty cycle = 6/3) and substrate holder temperature T = 400 °C. Prior to diamond growth, reference Si substrates were ultrasonically seeded in an aqueous suspension with detonation diamond powder (~5 nm). In the case of Si/MoS_2 samples, only half of the sample was nucleated, while the remaining area was kept as untreated. It should be noted that the samples were immersed only in an aqueous solution with diamond nanoparticles (without the application of ultrasound) to exclude possible mechanical damage to the MoS_2 layers already before the CVD process.

The surface morphology of the fabricated samples was analyzed using a field-emission scanning electron microscope (SEM) operating in secondary electron mode (MAIA3, Tescan Ltd.) or FEI Quanta 250 FEG-SEM. Raman spectra were acquired by Renishaw InVia Reflex Raman spectrometer equipped with He-Cd laser with an excitation wavelength of 442 nm or by a confocal Raman microscope (Alpha 300R, WiTec, Germany) using a 532 nm excitation laser wavelength.

Energy-dispersive X-ray spectra (EDX) were obtained using a dual-beam SEM combined with a high current focused ion beam - FEI Quanta 3D 200i equipped with EDS AMETEK (Oxford). EDX spectra were collected with an accelerating voltage of 10 kV, an emission current of 0.1 nA and a working distance of 10 mm.

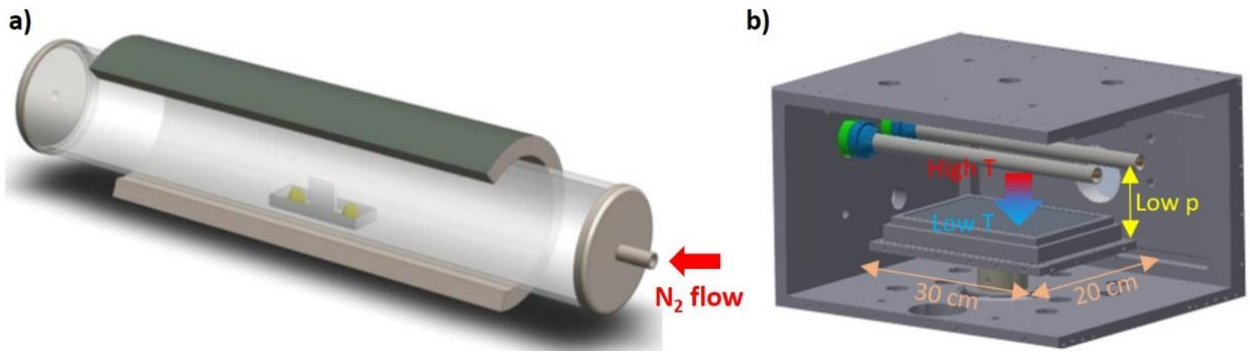

Figure 1 Schematic representation of the **a)** one-zone sulfurization method and **b)** pulsed MW plasma CVD system with a linear antenna arrangement (Roth&Rau AK400) [4,11].

3. RESULTS AND DISCUSSION

3.1. Growth and characterization of reference MoS_2 and diamond films

First, reference MoS_2 and diamond films were grown on Si substrates. **Figure 2** shows top-view SEM images and Raman spectra of MoS_2 film and diamond films deposited at two different gas compositions. The morphology of the MoS_2 film is characterized by a smooth surface with a small number of separated mounds.

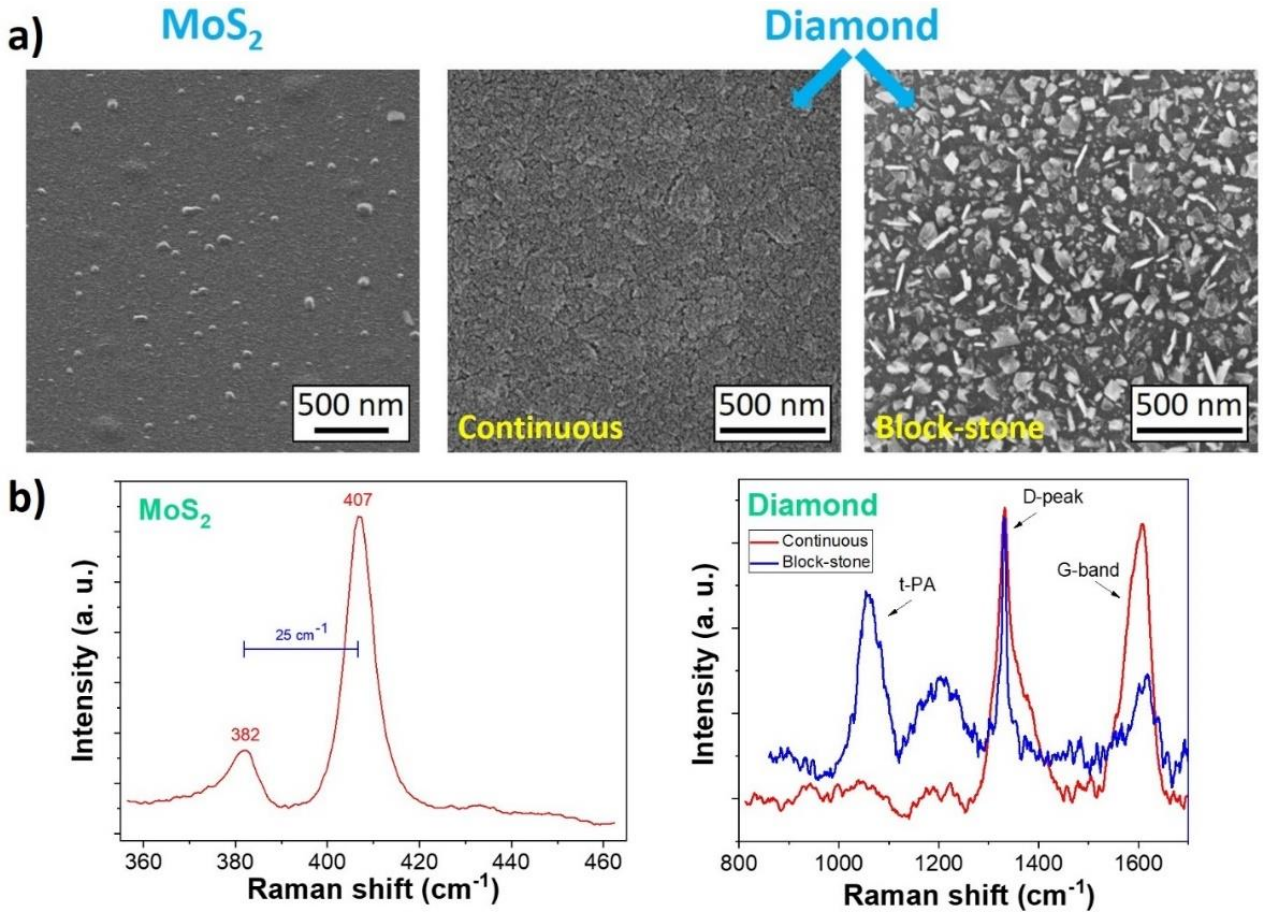

Figure 2 a) Top-view SEM images and **b)** Raman spectra of the deposited MoS_2 film and diamond films deposited in a linear antenna PE CVD system at two different gas compositions.

Raman measurements confirmed the MoS_2 character of the deposited film, with two dominant peaks in the spectrum corresponding to E^1_{2g} (382 cm^{-1}) and A^1_{1g} (407 cm^{-1}) Raman modes of MoS_2. In this case, the peak-to-peak (E^1_{2g} and A^1_{1g}) distance is more than 25 cm^{-1}, indicating that the film has more than 8 monolayers [12]. Based on results from the polarized Raman spectroscopy (not shown here), a horizontal alignment of the MoS_2 layer was confirmed [13]. The thickness of the MoS_2 film was about 18 nm, as measured by AFM.

Diamond films grown at two different gas compositions resulted in films with different morphologies, i.e. a continuous nanocrystalline film and a discontinuous layer consisting of individual well-faceted block-stone diamond crystals. The root-mean-square (RMS) surface roughness of the films was 7 nm and 40 nm, respectively. For both diamond films, a distinct peak (D-peak) centered at 1 332 cm^{-1} confirms the sp^3-bonded diamond character of the film. Moreover, the Raman spectrum of the continuous nanocrystalline diamond film also reveals the presence of a trans-polyacetylene chains (t-PA) at 1 150 cm^{-1} and a broad graphite band (G-band) at 1 450−1 650 cm^{-1} attributed to sp^2-bonded carbon. These non-diamond phases are usually localized at the diamond grain boundaries, which confirms the polycrystalline character of the diamond film.

3.2. Growth of MoS_2 on diamond

Figure 3a shows the surface morphologies of diamond films coated with MoS_2 layers. As found, the MoS_2 growth process does not damage the initial diamond films. The MoS_2 layers just copy the primary diamond surface morphology (the RMS roughness trend is similar to the reference diamond films). However, it should be noted that this is not at all the case when the diamond surface roughness is too high (e.g. in the case of a microcrystalline diamond, a shadowing effect may occur) or if the diamond film has a porous nature with a high-aspect-ratio. Due to the diamond surface roughness (RMS values are close to or higher than the MoS_2 thickness itself), it is not possible to evaluate the thickness and/or homogeneity of the grown MoS_2 film. Concerning the chemical structure, Raman measurements (**Figure 3b**) confirmed the successful conversion of Mo to MoS_2 layers on both types of diamond films [14].

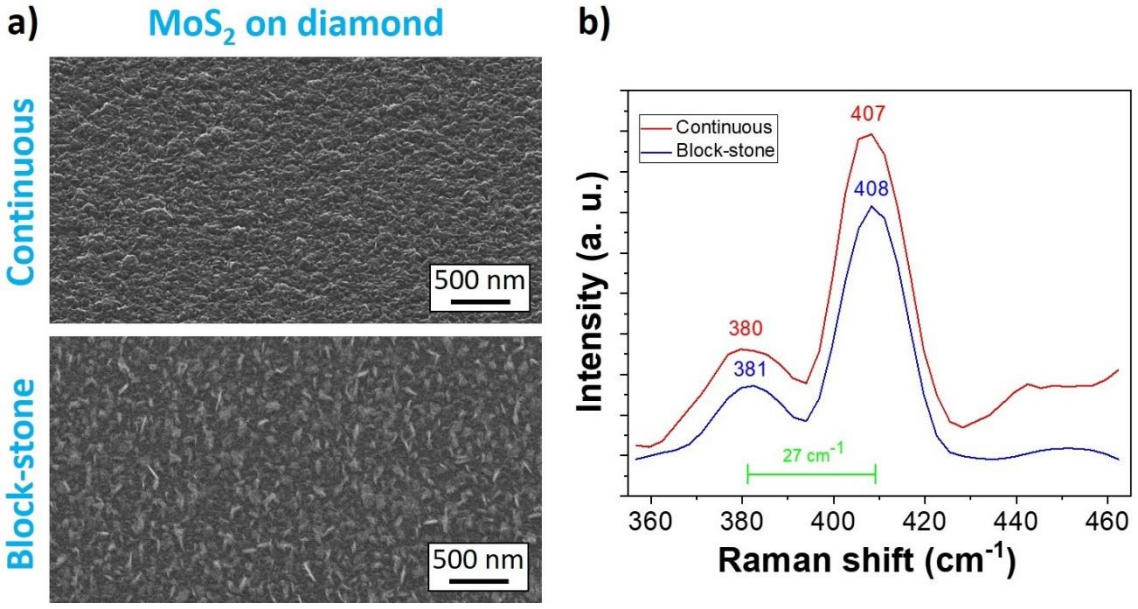

Figure 3 a) Top-view SEM images and **b)** Raman spectra of the fabricated heterostructure in the configuration MoS_2 on the continuous and block-stone diamond films.

3.3. Growth of diamond on MoS_2

The fabrication of MoS_2/diamond heterostructures was also carried out in the opposite way. To study the overall resistance of MoS_2 layers to the diamond CVD process, one-half of MoS_2/Si sample was nucleated,

and the remaining area was left untreated. **Figure 4a** shows an optical image of the boundary area between the nucleated and non-nucleated regions after the diamond growth. The nucleated region is clearly overgrown with a continuous nanocrystalline diamond film (as confirmed by Raman measurements) and reveals the same morphology as the reference diamond film, **Figure 4b**-nucleated vs. **Figure 2a**. The non-nucleated region reveals a damaged-like surface with locally overgrown carbon-based deposits initialized by the spontaneous diamond nucleation. Raman measurements (**Figure 4c**) confirmed that the MoS_2 layer on the non-nucleated region survived the harsh plasma environment during the diamond growth. However, a significant broadening and blue-shift of the characteristic peaks was observed. The MoS_2 layer under the diamond film was not clearly recognized by Raman measurements, although some indications of MoS_2 peaks can be observed in the spectrum. The presence of MoS_2 in both regions was also studied by energy-dispersive X-ray spectroscopy (EDX) (**Figure 4d**). Although the K-lines of sulfur overlap strongly with the L-lines of molybdenum [15], the intensity of the molybdenum and sulfur lines is similar in both film regions (with and without diamond film). So, as a next step, a detailed characterization of the MoS_2 layer under the diamond film is required.

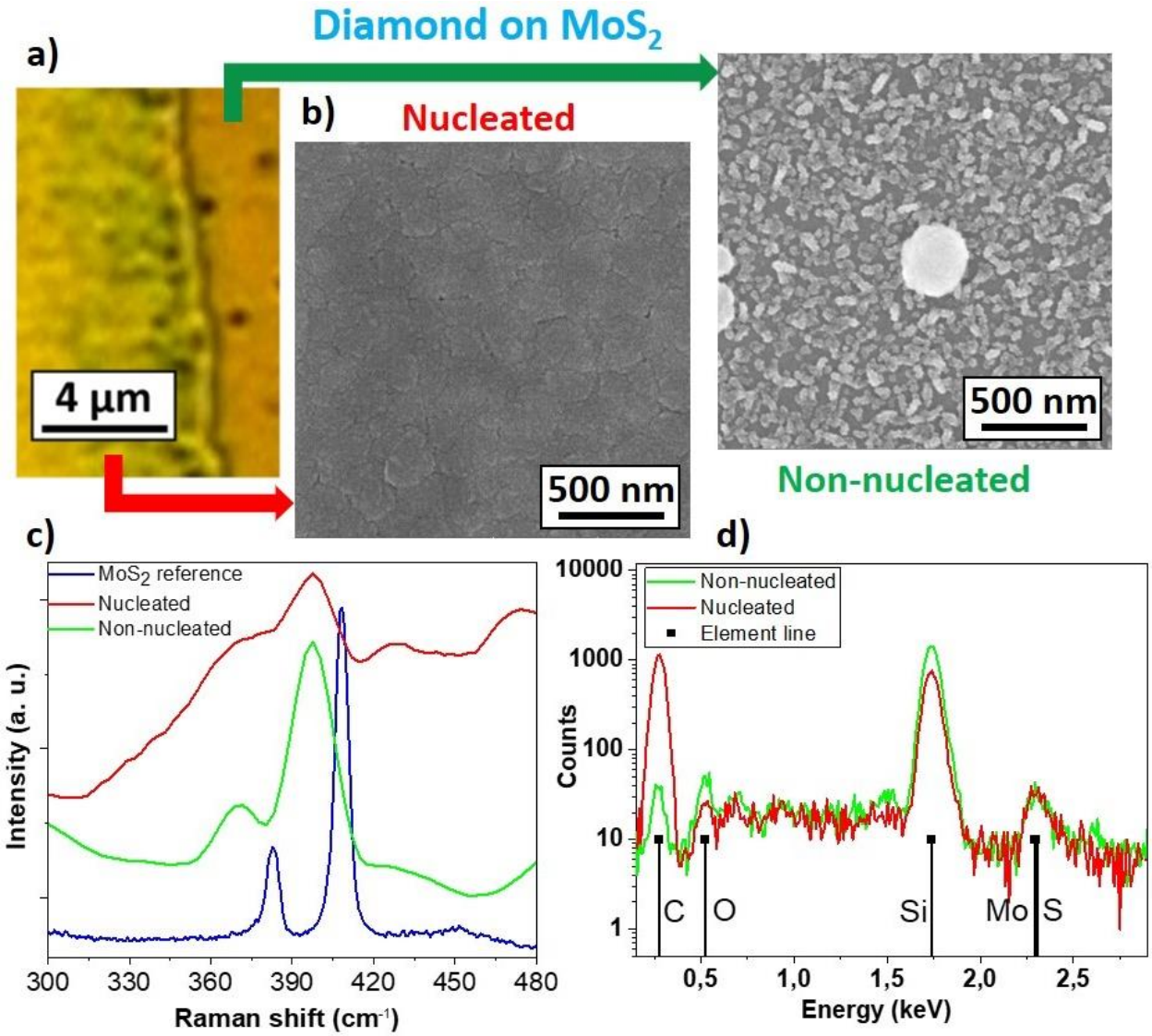

Figure 4 a) Optical image of the fabricated MoS_2/diamond heterostructure highlighted at the boundary of the nucleated and non-nucleated regions of the sample. **b)** Top-view SEM images, **c)** Raman spectra and **d)** EDX spectra of diamond films grown on nucleated and non-nucleated MoS_2 regions.

4. CONCLUSION

We investigated two technological concepts for the fabrication of MoS_2/diamond heterostructures. In the first concept, the diamond films were not damaged/modified with the MoS_2 growth process, and the formed MoS_2 layer well replicated the primary diamond morphology (continuous or porous). In the second concept, the MoS_2 film exposed to the diamond deposition conditions revealed some changes, as confirmed by Raman measurements. Some aspects of the diamond growth mechanism on the MoS_2 layer are still undiscovered and need deeper studies. Our preliminary results confirm technological progress in the fabrication of MoS_2/diamond heterostructures as a novel material platform attractive not only for fundamental research but also for industrially oriented applications.

ACKNOWLEDGEMENTS

This work was supported by project 19MRP0010 financed from the MoRePro program and funding from the Slovak Academy of Sciences, Slovak Grant Agency for Science VEGA 2/0059/21, bilateral GAAV project no. SAV-AV ČR 21-10 and project Lumina Queruntur of the Czech Academy of Sciences.

REFERENCES

[1] N. SHANTO, J.R. MCCARTHY, eds.. Biomedical applications of graphene and 2D nanomaterials. *Elsevier*. Amsterdam, 2019.

[2] A.K. GEIM, I.V. GRIGORIEVA. Van der Waals heterostructures. *Nature*. 2013, vol. 499, pp. 419–425. Available from: https://doi.org/10.1038/nature12385.

[3] H. TERRONES, F. LÓPEZ-URÍAS, M. TERRONES. Novel hetero-layered materials with tunable direct band gaps by sandwiching different metal disulfides and diselenides. *Sci Rep*. 2013, vol. 3, pp. 1549. Available from: https://doi.org/10.1038/srep01549.

[4] M. SOJKOVÁ, P. SIFFALOVIC, O. BABCHENKO, G. VANKO, E. DOBROČKA, J. HAGARA, N. MRKYVKOVA, E. MAJKOVÁ, T. IŽÁK, A. KROMKA, M. HULMAN. Carbide-free one-zone sulfurization method grows thin MoS2 layers on polycrystalline CVD diamond. *Sci Rep*. 2019, vol. 9, 2001. Available from: https://doi.org/10.1038/s41598-018-38472-9.

[5] M. SAMADI, N. SARIKHANI, M. ZIRAK, H. ZHANG, H.-L. ZHANG, A.Z. MOSHFEGH. Group 6 transition metal dichalcogenide nanomaterials: synthesis, applications and future perspectives. *Nanoscale Horiz*. 2018, vol. 3, pp. 90–204. Available from: https://doi.org/10.1039/C7NH00137A.

[6] J. WILKS, E. WILKS. Properties and applications of diamond. paperback ed, Butterworth-Heinemann, Oxford, 1994.

[7] M. DOMONKOS, M. VARGA, L. ONDIČ, L. GAJDOŠOVÁ, A. KROMKA. Microsphere lithography for scalable polycrystalline diamond-based near-infrared photonic crystals fabrication. *Materials & Design*. 2018, vol. 139, pp. 363–371. Available from: https://doi.org/10.1016/j.matdes.2017.10.076.

[8] A.G. MONTAÑO-FIGUEROA, J.J. ALCANTAR-PEÑA, P. TIRADO, A. ABRAHAM, E. DE OBALDIA, O. AUCIELLO. Tailoring of polycrystalline diamond surfaces from hydrophilic to superhydrophobic via synergistic chemical plus micro-structuring processes. *Carbon*. 2018, vol. 139, pp. 361–368. Available from: https://doi.org/10.1016/j.carbon.2018.06.062.

[9] P. YU, Y.-H. CHU, R. RAMESH. Oxide interfaces: pathways to novel phenomena. *Materials Today*. 2012, vol. 15, pp. 320–327. Available from: https://doi.org/10.1016/S1369-7021(12)70137-2.

[10] A. GALASHEV, K. IVANICHKINA. Computer study of the structure and thermal stability of a monolayer MoS2 film on a diamond substrate. *Lett. Mater*. 2019, vol. 9, pp. 270–275. Available from: https://doi.org/10.22226/2410-3535-2019-3-270-275.

[11] M. VARGA, Š. POTOCKÝ, M. DOMONKOS, T. IŽÁK, O. BABČENKO, A. KROMKA. Great Variety of Man-Made Porous Diamond Structures: Pulsed Microwave Cold Plasma System with a Linear Antenna Arrangement, *ACS Omega.* 2019, vol. 4, pp. 8441–8450. Available from: https://doi.org/10.1021/acsomega.9b00323.

[12] G. SIEGEL, Y.P. VENKATA SUBBAIAH, M.C. PRESTGARD, A. Tiwari, Growth of centimeter-scale atomically thin MoS_2 films by pulsed laser deposition. *APL Materials*. 2015, vol. 3, 056103. Available from: https://doi.org/10.1063/1.4921580.

[13] M. HULMAN, M. SOJKOVÁ, K. VÉGSÖ, N. MRKYVKOVA, J. HAGARA, P. HUTÁR, P. KOTRUSZ, J. HUDEC, K. TOKÁR, E. MAJKOVA, P. SIFFALOVIC. Polarized Raman Reveals Alignment of Few-Layer MoS_2 Films. *J. Phys. Chem. C*. 2019, vol. 123, pp. 29468–29475. Available from: https://doi.org/10.1021/acs.jpcc.9b08708.

[14] K. GOŁASA, M. GRZESZCZYK, R. BOŻEK, P. LESZCZYŃSKI, A. WYSMOŁEK, M. POTEMSKI, A. BABIŃSKI. Resonant Raman scattering in MoS 2 —From bulk to monolayer. *Solid State Communications*. 2014, vol. 197, pp. 53–56. Available from: https://doi.org/10.1016/j.ssc.2014.08.009.

[15] E. NOLOT, S. CADOT, F. MARTIN, P. HÖNICKE, C. ZECH, B. BECKHOFF. In-line characterization of ultrathin transition metal dichalcogenides using X-ray fluorescence and X-ray photoelectron spectroscopy. *Spectrochimica Acta Part B: Atomic Spectroscopy.* 2020, vol. 166, 105788. Available from: https://doi.org/10.1016/j.sab.2020.105788.